Fabrication of a colorimetric sensor using acetic acid-capped drug-mediated copper oxide nanoparticles for nitrite biosensing in processed food

Umar Nishan[1]*, Sajida Rehman[1], Riaz Ullah[2], Ahmed Bari[3],
Saifullah Afridi[1], Mohibullah Shah[4], Jibran Iqbal[5],
Muhammad Asad[1], Amir Badshah[1], Naeem Khan[1], In Min Hwang[6],
Hameed Ullah Khan[1] and Nawshad Muhammad[7]*

[1]Department of Chemistry, Kohat University of Science and Technology, Kohat, Pakistan, [2]Department of
Pharmacognosy, College of Pharmacy, King Saud University, Riyadh, Saudi Arabia, [3]Department of
Pharmaceutical Chemistry, College of Pharmacy, King Saud University, Riyadh, Saudi Arabia, [4]Department
of Biochemistry, Bahauddin Zakariya University, Multan, Punjab, Pakistan, [5]College of Natural and Health
Sciences, Zayed University, Abu Dhabi, United Arab Emirates, [6]Fermentation Regulation Research Group,
World Institute of Kimchi, Gwangju, Republic of Korea, [7]Department of Dental Materials, Institute of Basic
Medical Sciences, Khyber Medical University, Peshawar, Pakistan

Nitrite (NO_2^-) and nitrate (NO_3^-) are frequently used in cured meat products as
preservatives, as they give a better taste and work well in color fixation. As a key
possible carcinogen, excessive dietary consumption of NO_2^- in cured meat
products would be bad for health. Herein, copper oxide nanoparticles (CuO
NPs) were synthesized using the drug Augmentin as a reducing and capping
agent. The desired synthesis of CuO NPs was confirmed by various
characterization techniques, including UV−visible spectroscopy, Fourier
transform infrared spectroscopy, energy-dispersive X-ray spectroscopy,
thermal gravimetric analysis, X-ray diffraction, and scanning electron
microscopy. The new approach of drug-mediated acetic acid-capped CuO
NPs was developed for simple colorimetric detection of nitrite ions in a mimic
solution of processed food. The color of the detection system changes from
brown to yellow with the increase in the concentration of NO_2^- and has been
observed with the naked eye. The selectivity of the NO_2^- detection system by the
UV−visible spectrum and the naked eye is compared to other ions, such as Br^-, I^-,
Cl^{-1}, PO_4^{-3}, CO_3^{2-}, and SO_4^{2-}. The platform was successfully employed for the
determination of nitrite in real samples. Moreover, this probe can be used for the
sensitive detection of NO_2^- with a linear range of 1×10^{-8} to 2.40×10^{-6} M, a
detection limit of 2.69×10^{-7} M, a limit of quantification 8.9×10^{-7} M, and a
regression coefficient (R^2) of 0.997. Our results suggest that this sensor can be
used for on-site analysis and quantification as well as in the fields of disease
diagnosis, environmental monitoring, and food safety.

KEYWORDS

Augmentin drug, CuO NPs, cured meat samples, biosensor, interference study, nitrite

1 Introduction

Among nitrogen-containing inorganic ions, three ions, i.e., NH_4^+, NO_2^-, and NO_3^-, in the environment are essential nutrients for the growth of plants and in the food industry (Flores and Toldrá, 2021). Sodium and potassium salts of nitrite and nitrate have long been used in the meat industry as food preservatives. They work by prolonging the shelf life of processed meat, giving it a better taste, and fixing its color (Majou and Christieans, 2018). Nitrite is more frequently detected in groundwater than in surface water. Livestock waste, artificial fertilizers, and erosion of natural deposits are its main sources (Greer et al., 2005). The Environmental Protection Agency (EPA) of the United States has defined the maximum contamination level (MCL) of nitrite in drinking water and food products to be 21.7 mM (Ozdestan and Uren, 2010) and 125 mg/kg, respectively (Singh et al., 2019). The excess intake of NO_2^- reported different medical issues, such as birth defects and methemoglobinemia, commonly known as blue baby syndrome (Brender, 2020), affecting the nervous system (Wang et al., 2016), spleen, and kidneys, and also causing esophageal cancer (Ozdestan and Uren, 2010). Due to the strong reactivity of nitrite, rapid and accurate analytical techniques are required to reduce human health risks. It is vital to identify and monitor the NO_2^- concentration of food products and environmental, organic, and inorganic samples.

Carboxylic acids are the most common organic compounds and belong to the class of green solvents, possessing no or low toxicity and being relatively inexpensive (Teles et al., 2017). They have significant applications in the petrochemical, food, dye, and stabilizer industries, as well as in nanotechnology (Odedairo et al., 2013). In addition to stabilizing nanoparticles, they can also affect the solubility, reactivity, size, and shape of nanoparticles, as well as the surface modification of nanostructures (Sarkar et al., 2005). Carboxylic acids are used as stabilizers because they can easily coordinate with the surface of nanoparticles (Hosseini-Monfared et al., 2015). Moreover, the functionalization of nanoparticles with the carboxylic group produces more active sites for sensing (Sáenz-Galindo et al., 2018).

Numerous methods have been employed to detect nitrite, such as chromatographic (Lim et al., 2022), chemiluminescence (Basu et al., 2022), electroanalytical (Gao et al., 2020), and spectrophotometric methods (Karrat et al., 2022). However, the aforementioned analytical techniques have some limitations when used on a daily basis for nitrite detection. Due to complicated sample preparation procedures, expensive and complicated instruments, and highly trained operators, these techniques have become undesirable in laboratories, especially with limited financial resources. Therefore, it is desirable to develop such techniques, which could be more efficient, more fruitful, and less expensive. Usually, scientists try to translate the analyte signals into colors, which can be easily detected with the naked eye. A very simple and cheap colorimetric sensor is particularly attractive for nitrite detection in food and water samples (Zhang et al., 2012). Simple, cost-effective design, and quick response are the cornerstones of colorimetric sensors (Nishan et al., 2021a). Prior to becoming a bulky and complicated device, a sensor's various functional components, such as the transducer, recycling unit, and discovery unit, were crucial to a delayed detector response (Cheng et al., 2014). Recently, electrocatalyst materials have played important roles in colorimetric sensors due to their desirable characteristics, including strong surface plasmon resonance and distance-dependent optical properties, as well as the fact that their performance events may be seen with the naked eye (Nishan et al., 2021b). Currently, a number of electrocatalytic materials, including metallic oxides, carbon nanomaterials, and metal nanomaterials, have been employed to create nitrite sensors (Lin et al., 2011; Wang et al., 2014).

For the colorimetric detection of nitrite, various nanomaterials have been reported, such as Au NPs-rGO (Amanulla et al., 2017), Ag/Au NPs (Li et al., 2015), MTT-G NPs (Nam et al., 2014), Au NPs (Ye et al., 2015), Er_2O_3 NPs@RGO (Rajaji et al., 2019), $Fe_3O_4@SiO_2$/Au magnetic nanoparticles (Chen et al., 2016), shell-isolated nanoparticles (Zhang et al., 2013), Pd NPs (Pourreza and Abdollahzadeh, 2019), Ag NPs (Kumar and Anthony, 2014), Fe_3O_4/MWCNTs (Qu et al., 2015), AuNP–CeO_2 NP@GO (Adegoke et al., 2021), and MnO_2 NPs (Nishan et al., 2022). Compared to different inorganic oxides, such as V_2O_5, NiO, and Co_3O_4, copper oxide nanoparticles (CuO NPs) have gained much attention because of their low cost, availability, and lack of toxicity (Jaiswal et al., 2017). CuO NPs are exceptional materials for the optical detection of nitrite due to their surface plasmon properties.

The current research reports the drug-mediated production of CuO nanostructures *via* using the Augmentin drug as a reducing and stabilizing agent. It is the first study on the production of CuO NPs *via* drug-mediated means without the need for any additional reduction agents. Furthermore, to overcome the problem of agglomeration of the nanoparticles and the availability of surface area for reactions, acetic acid has been employed as a deagglomerating and capping agent. The platform of acetic acid-capped CuO NPs has been successfully used as a colorimetric sensor for the detection of nitrite. Comprehensive optimization of various parameters, such as loading of nanoparticles, pH, reaction time, and concentration of nitrite, was carried out. The sensing platform was also successfully applied to real samples.
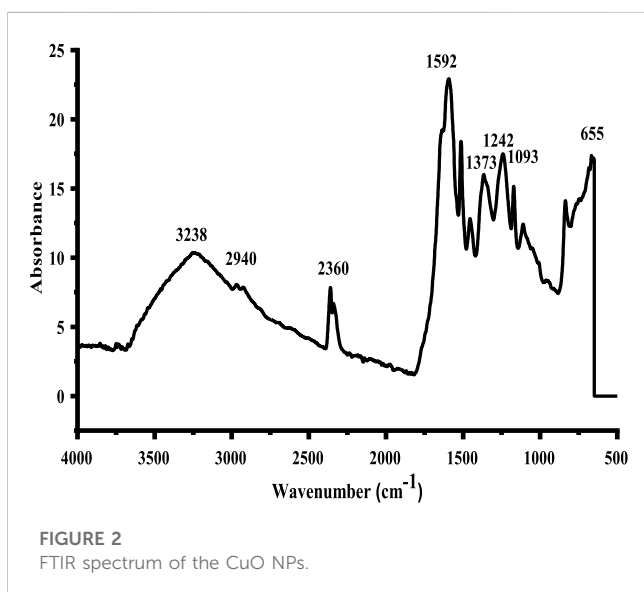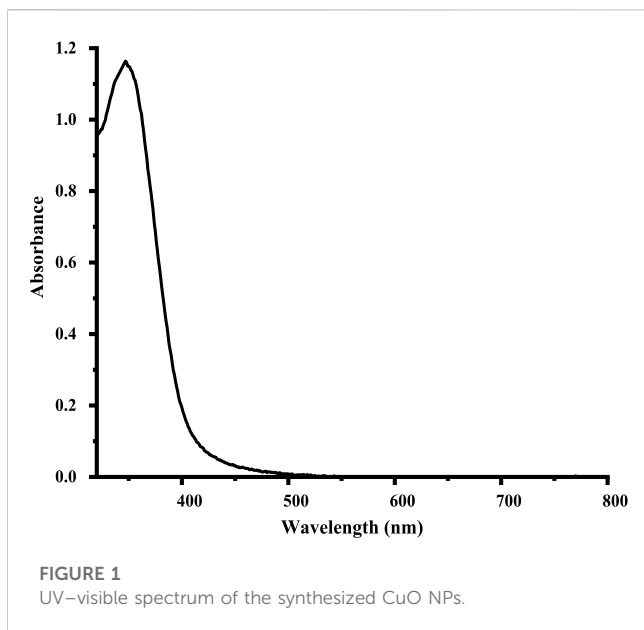
2 Experimental

2.1 Reagents

All the required chemicals, including acetic acid (CH_3COOH, 98.4%), copper sulfate ($CuSO_4$, 99.4%), and sodium nitrite ($NaNO_2$, 98.2%), were analytical-grade reagents and were purchased from Sigma-Aldrich, and 1 g of Augmentin drug tablets (GSK) were purchased from a local medical store.

2.2 Instrumentation

An FTIR spectrometer (Agilent Technologies, Danbury, Connecticut, United States) was used to observe the characteristic peaks of CuO NPs. Samples were analyzed for their thermal stability by simultaneous thermal analysis (STA) (PerkinElmer, Waltham, Massachusetts, United States) and thermal gravimetric analysis (TGA) at temperatures ranging from 30°C–800°C. An energy-dispersive X-ray spectrometer (EDX) (Model JSM 6390)

FIGURE 1
UV–visible spectrum of the synthesized CuO NPs.

FIGURE 3
XRD pattern of the synthesized CuO NPs.

FIGURE 2
FTIR spectrum of the CuO NPs.

was used for the confirmation of the chemical composition of the synthesized CuO NPs (SEM–EDS) with a TESCAN VEGA (LMU) SEM with INCAx-act (Brno, Czech Republic). X-ray diffraction was used for the analysis and phase identification of CuO NPs (Shimadzu, Kyoto, Japan, LabX XRD-6100) with Cu-Kα radiation at a scan range of 10°C–80°C. Absorption spectra were measured through UV–visible spectroscopy (Agilent Shimadzu, UV-1800, Kyoto, Japan).

2.3 Synthesis of CuO NPs

Two 1 g Augmentin tablets were mechanically ground into a fine powder, and 50 mM of Augmentin solution was prepared
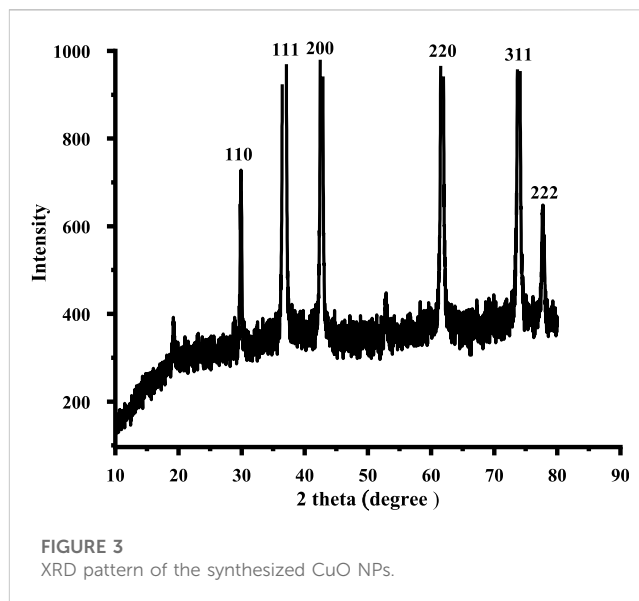
(50 mL) in distilled water followed by filtration. The clear filtrate was added to the 50 mM copper nitrate solution dropwise for 5 h under stirring, and the solution was centrifuged for 15 min at 4,000 rpm at 4°C. The prepared nanoparticles were kept in an oven for drying at 50°C for 4 h. The dried nanoparticles were kept in an Eppendorf tube at room temperature for further use (Nishan et al., 2020; Asad et al., 2022).

2.4 Deagglomeration of CuO nanostructures with acetic acid

Copper oxide nanoparticles were coated with acetic acid. Acetic acid has been used as a dispersion medium and stabilizing agent to avoid the agglomeration of the nanoparticles. In this process, 1 mL of acetic acid and 6 mg of copper oxide nanoparticles were combined and stirred for 30 min with a glass rod for uniform dispersion. The acquired mixture of copper oxide nanoparticles coated with acetic acid was stored and used for the colorimetric detection of nitrite. One of the methods used is to cover colloids with a protective agent that may be bound to the surface of the particles in order to keep the nanoparticles suspended and, thus, prevent aggregation (Deng et al., 2013).

2.5 Colorimetric detection of nitrite

For the colorimetric detection of nitrite ions, the reaction was conducted at ambient temperature and in acidic media. For the proposed assay, 100 μL of nitrite solution (2.4×10^{-6} M) and 100 μL of CH_3COOH-capped copper oxide nanoparticles were taken in an Eppendorf tube at room temperature. After the addition of nitrite solution, the brown color of the acetic acid-coated copper oxide nanoparticles changed into a light yellow color. The proposed assay response was observed with the naked eye and also assessed using a UV–Vis spectrophotometer.
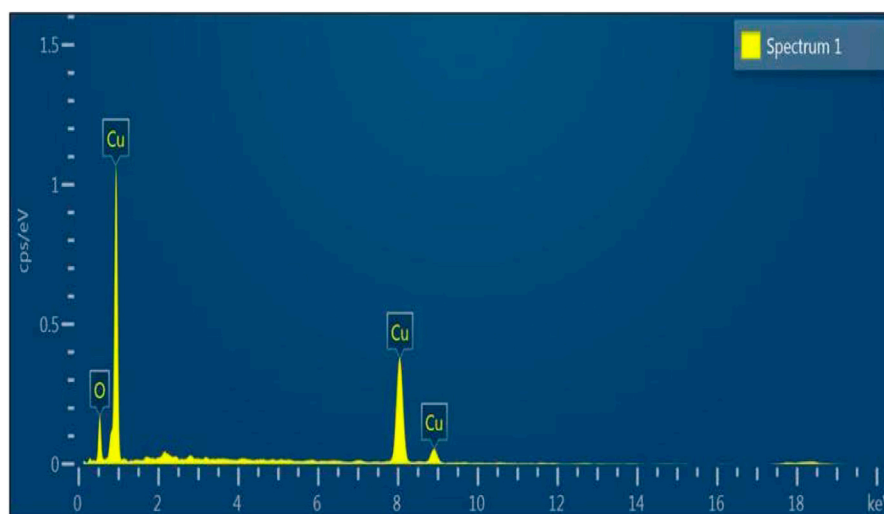
FIGURE 4
EDX analysis of the synthesized CuO NPs.

TABLE 1 EDX analysis.

Element	Line type	Weight %	Weight % sigma	Atomic %
Cu	K series	88.67	1.65	66.33
O	K series	11.33	1.65	33.67
Total		100.00		100.00

3 Results and discussion

3.1 Characterization of CuO NPs

Prior to the investigation of the potential sensing application of the proposed CuO NPs, it was characterized by the following techniques.

3.1.1 UV–Vis spectrophotometry

The UV–visible spectrum of the synthesized CuO NPs is shown in Figure 1. The recorded main peak at 350 nm is consistent with the literature-reported values of corresponding CuO NPs (Fernández-Arias et al., 2020).

3.1.2 The synthesized nanostructures' FTIR analysis

The produced nanoparticles' FTIR spectrum is depicted in Figure 2. FTIR confirms the existence of various functional groups. The broad band in the region of 3,238–2,500 cm^{-1} indicated the presence of the OH group of the carboxylic group. The band at 1,592 cm^{-1} is assigned to the C–O stretching vibrations of the carboxylic group. The 1,242 cm^{-1} and 1,373 cm^{-1} absorption band regions were assigned to C–N bending vibration and S = O stretching, respectively. The absorption band in the 655 cm^{-1} region indicated a Cu–O stretching vibration, confirming the formation of CuO NPs (Ethiraj and Kang, 2012).

3.1.3 XRD analysis

The XRD pattern shows the high crystalline nature of the drug-induced CuO NPs with prominent sharp peaks, as shown in Figure 3. The diffraction peaks ascribed to the Miller indices 110, 111, 200, 220, 311, and 222.68 at 2Ө are 29.86°C, 36.58°C, 42.60°C, 61.84°C, 73.85°C, and 77.68°C. The XRD analysis shows the peculiar purity of CuO NPs with no additional peaks. By using the Debye–Scherrer equation, the average crystalline size of CuO NPs is 22 nm. The findings were intimately associated with the results for nanoparticles of cuprous oxide (Shi et al., 2019).

3.1.4 EDX analysis

Figure 4 displays the produced nanoparticles' EDX spectrum. The EDX of the copper oxide nanoparticles spectrum indicates that the weight composition of copper and oxygen is 87.2% and 12.72%, respectively. The EDX spectrum with no other peak reflects the high purity of the synthesized copper oxide nanoparticles. The elemental analysis is shown in Table 1. The EDX results are in good conformity with the available literature for CuO nanoparticles (Hosseini-Koupaei et al., 2019).

3.1.5 TGA analysis

The thermal stability of the copper oxide nanoparticles was confirmed by TGA, as shown in Figure 5. The first TGA curve between 100°C–150°C curve shows a 0.7 percent loss in weight,
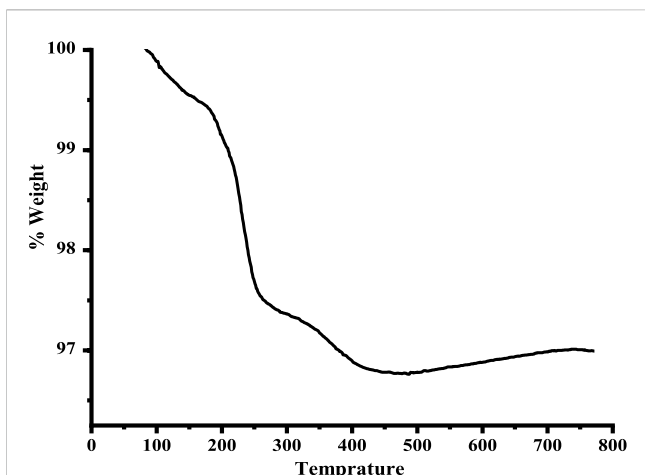
FIGURE 5
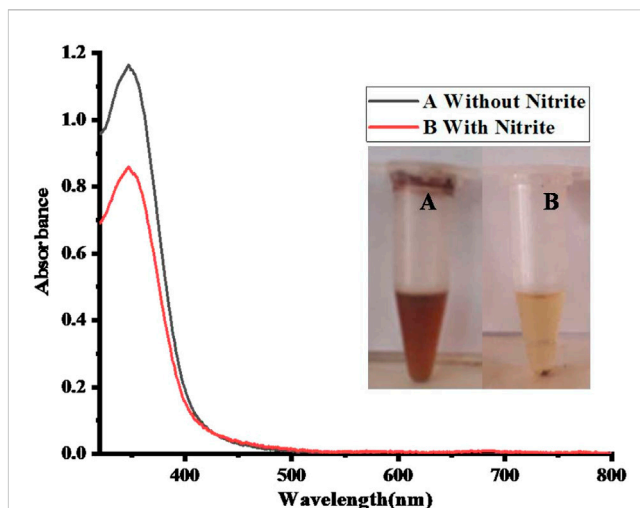TGA investigation of the prepared CuO nanostructures.

FIGURE 7
UV−Vis spectra of **(A)** 100 μL of CH$_3$COOH-capped CuO nanoparticles without nitrite **(B)** in the presence of 100 μL of nitrite solution (2.4 × 10^{-6} M).
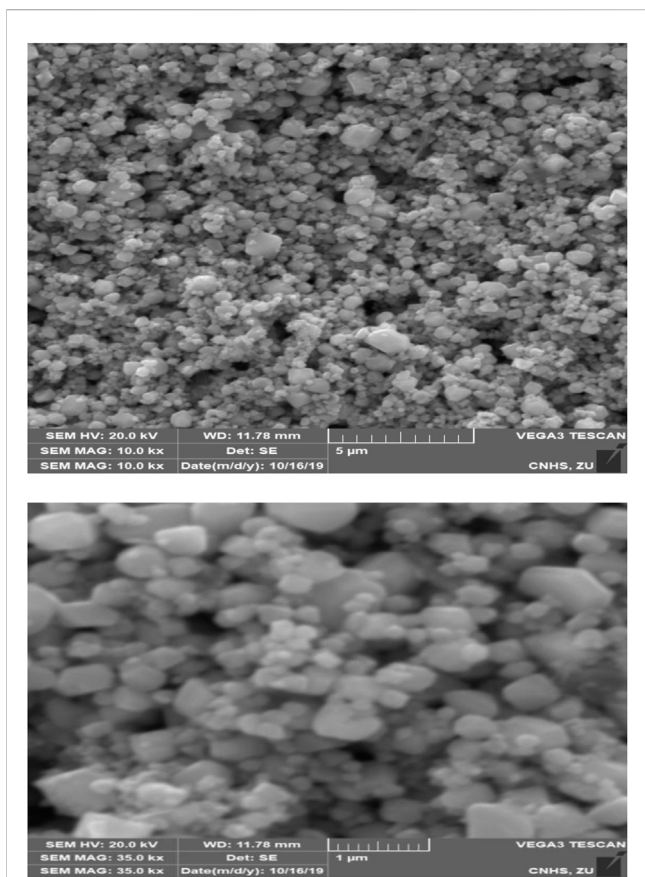

FIGURE 6
SEM photographs of the produced CuO NPs.

FIGURE 8
Optimization of acetic acid-capped CuO NPs in (μL). The best response was observed at point E, with reaction conditions [100 μL of capped CuO NPs and 100 μL of nitrite solution (2.40 × 10^{-6} M)]. Points **(A-F)** represents the absorbance changes in response to different amounts of capped CuO NPs.

3.1.6 SEM analysis

Figure 6 shows the SEM images of the cross-section of the prepared CuO NPs. SEM images confirm the morphology of the prepared nanoparticles. The SEM images clearly show that due to the agglomeration propensity, the nanoparticles are formed in cubical, crystalline, and clustered forms and are compatible with the cited literature (Lanje et al., 2010).

3.2 Colorimetric detection of nitrite

Acetic acid-coated CuO NPs have been used as a sensing platform for the colorimetric detection of nitrite. For the sensing of nitrite, 100 μL of CH$_3$COOH-capped CuO nanoparticles were

indicating the loss of water, while the loss of organic moieties is in the range of 170°C–250°C, with a weight loss of 2.7 percent. Owing to the surface oxidation reactions taking place in the reacting atmosphere, the curve also shows weight gain in the sample (Loganathan et al., 2017).
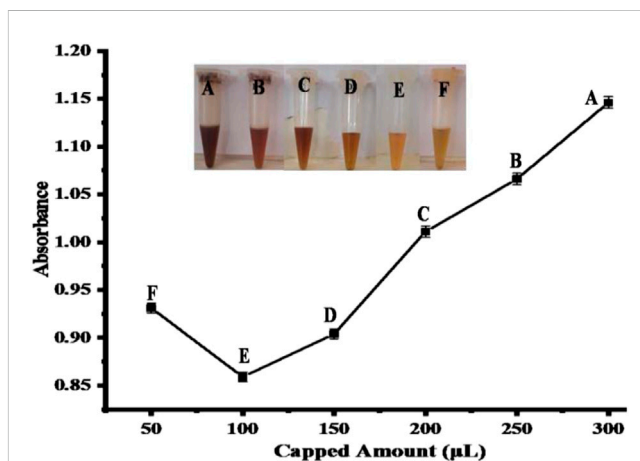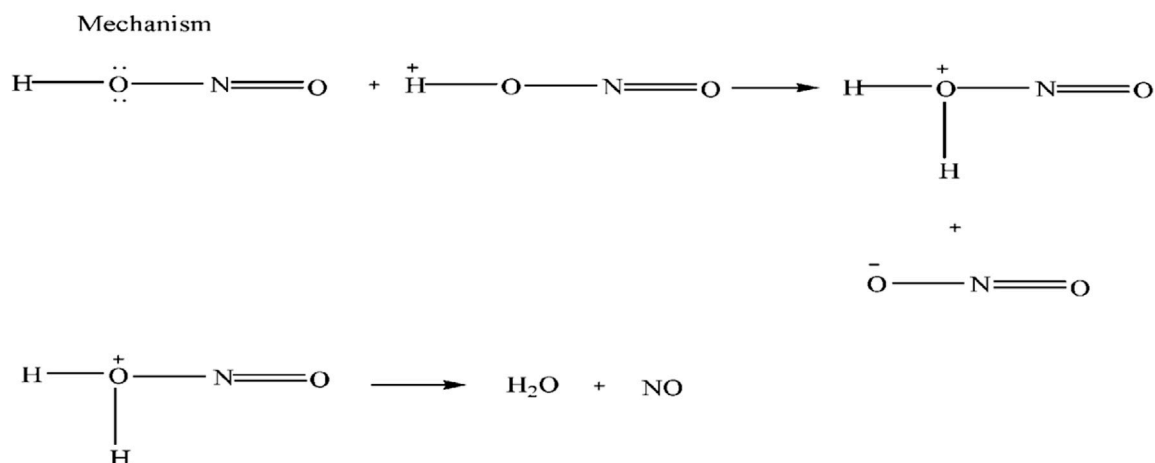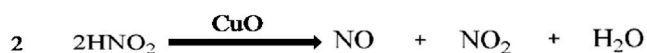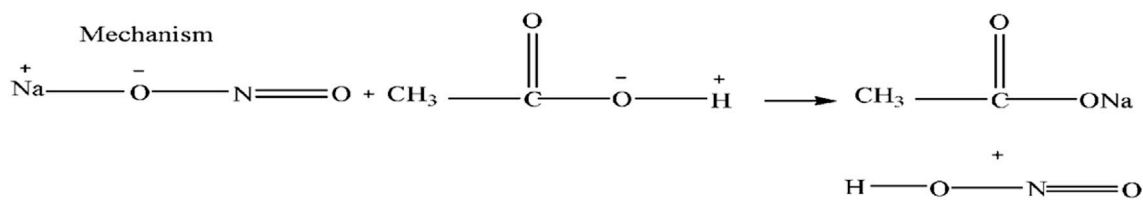
SCHEME 1
Proposed mechanism.
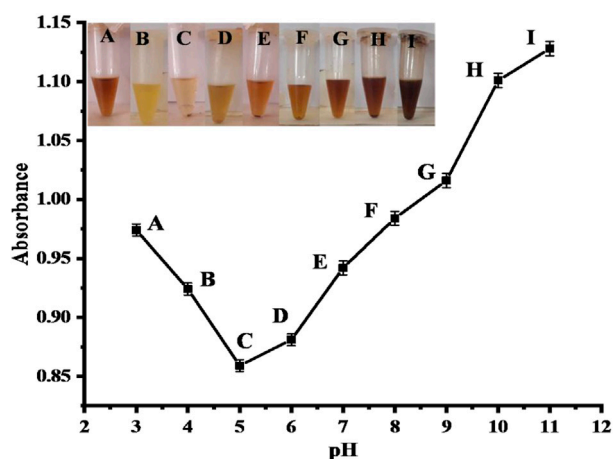
FIGURE 9
Optimization of pH. Point C (pH 5) shows a good response with [CH$_3$COOH-coated CuO nanoparticles = 100 μL] [nitrite = 2.40 × 10^{-6} M (100 μL)] reaction conditions. Points (A-I) represents the absorbance changes in response to change in pH.

FIGURE 10
Time optimization. Point D (4 min) shows a good response with [CH$_3$COOH-coated CuO nanoparticles = 100 μL] [nitrite = 2.40 × 10^{-6} M (100 μL)] reaction mixture conditions. The inset figure displays the colorimetric changes with time. Points (A-F) represents the absorbance changes in response to change in time.

mixed with an equal volume (100 μL; 2.4 × 10^{-6} M) of sodium nitrite solution. The process was carried out at an ambient temperature, resulting in the color changing from brown to yellow after adding nitrite solution, as shown in Figure 7. The absorption spectra of the proposed assay were recorded using a UV–Vis spectrophotometer, as shown in Figure 7.

FIGURE 11
Biosensing of NO_2^-. **(A)** UV−Vis spectra and the resulting change with respect to the change in different nitrite concentrations. **(B)** Nitrite concentration versus absorbance calibration graph.

3.3 Potential method of CuO NP-based nitrite detection

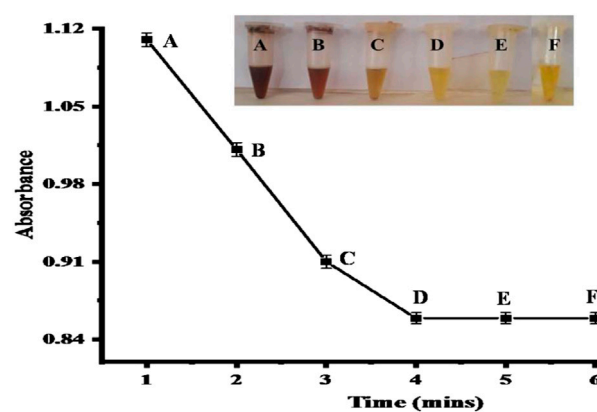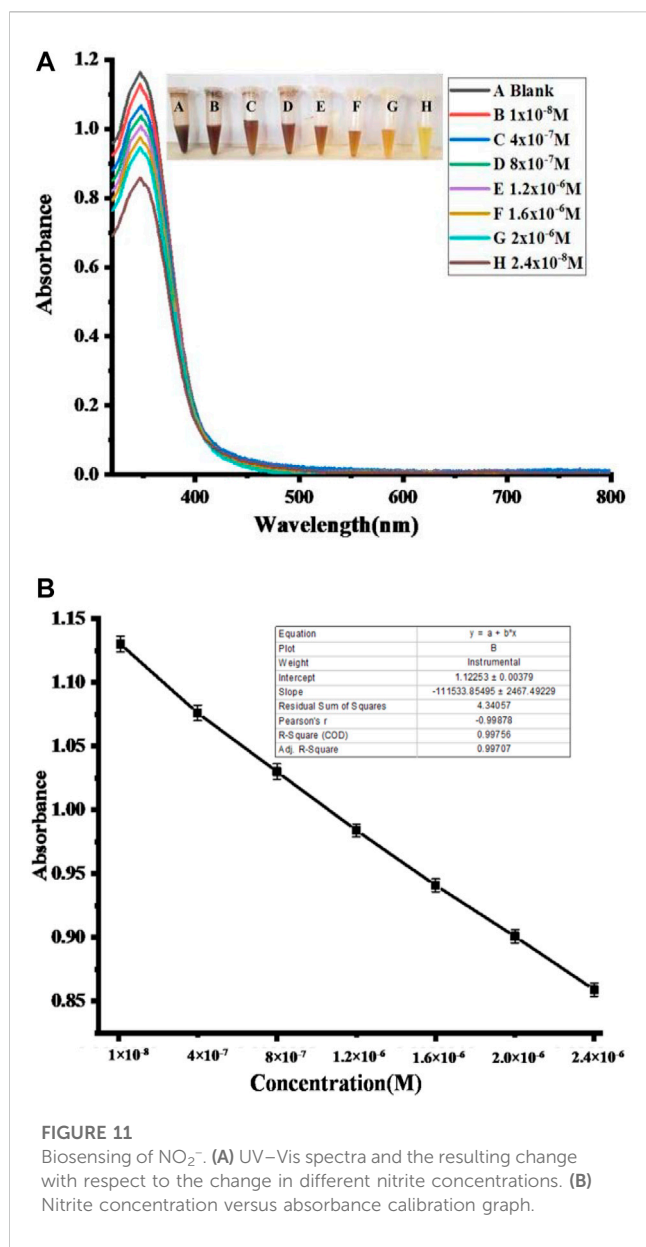The suggested mechanism for nitrite sensing by the well-characterized acetic acid-coated CuO NPs is shown in Scheme 1. In brief, the acetic acid-coated CuO NPs reduce the sodium nitrite salt into sodium acetate and nitrite acid (as shown in reaction 1). Then, the nitrite acid is oxidized into NO and NO_2 in the presence of CuO (as shown in reaction 2), resulting in the color changing to yellow.

3.4 Optimization of various factors affecting the parameters

3.4.1 Effect of copper oxide nanoparticle loading

Normally, colloids of nanoparticles appear to aggregate in a solution. In order to keep the nanoparticles suspended and prevent them from aggregating, one of the strategies is to cover colloids with a protective agent that can be associated with the surface of the particle (Sun and Luo, 2005). Acetic acid serves as a stabilizing agent in the present work. Visual color change was observed in the colorimetric approach using copper oxide nanoparticles. To obtain the best colorimetric response of the proposed sensor, different amounts of acetic acid-capped nanoparticles (50–300 μL) were used. The color of the solution does not improve at a higher concentration of nanoparticle dispersion with 100 μL of nitrite ions (2.4×10^{-6} M); it remains brown because the analyte cannot completely bind to the surface of the nanoparticles. As the amount of dispersion decreases, the color slowly changes from brown to yellow. In nanoparticle dispersion at 100 μL, the colorimetric detection of nitrite was clearly seen by the naked eye, where the dark brown color changed to a yellow color along with the bubbles of nitric oxide gas formation. The solution of nitrite ions in 100 μL interacts promptly with the dispersion of CH_3COOH-coated copper oxide nanoparticles in 100 μL, as shown in Figure 8.

3.4.2 Effect of PH

The sensor's response was also evaluated at different pH ranges (3–11) using standard HCl and NaOH solutions for pH calibration in the fabrication of the proposed sensor, as shown in Figure 9. The proposed sensor's best response was observed at pH 5, which resulted

TABLE 2 Comparative analysis of the proposed assay with the previously reported studies.

| S. no.	Analytical method	Linear range (μM)	LOD (μM)	References
1	Hydrogel	10–5,000 μM	10 μM	Nam et al. (2018)
2	Gold nanoparticles	0–200	10	Ye et al. (2015)
3	Aza-BODIPY	0–20	0.5	Adarsh et al. (2013)
4	Ag@Au nanoparticles	1–20	4	Li et al. (2015)
5	Gold nanoparticles	0–174	10.8	Xiong et al. (2017)
6	Ag NPs	0–460	0.1	Kumar and Anthony (2014)
7	Au NPs–rGO nanocomposite	1–20	0.1	Amanulla et al. (2017)
8	Acetic acid-capped CuO NPs	0.01–2.40	0.2	This work
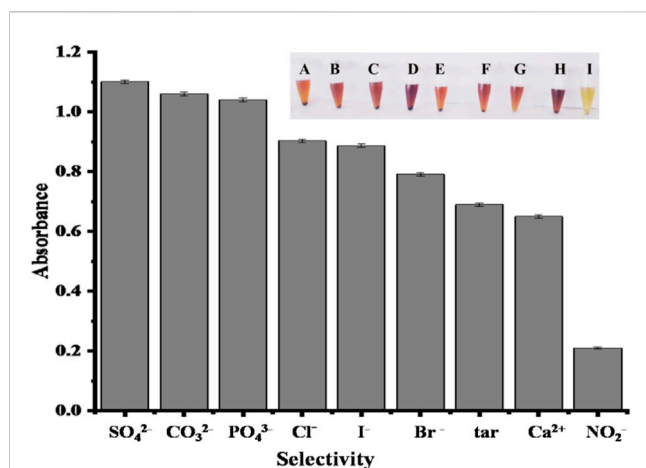
FIGURE 12
Biosensor selectivity of CH_3COOH-coated CuO nanoparticles for NO_2^- and the fabricated sensor with other co-existing ions at the same concentration (2.40×10^{-6} M), such as SO_4^{2-} **(A)**, CO_3^{2-} **(B)**, PO_4^{3-} **(C)**, Cl^- **(D)**, I^- **(E)**, Br^- **(F)**, tar **(G)**, Ca^{2+} **(H)**, and NO_2^- **(I)**, under optimum experimental conditions.
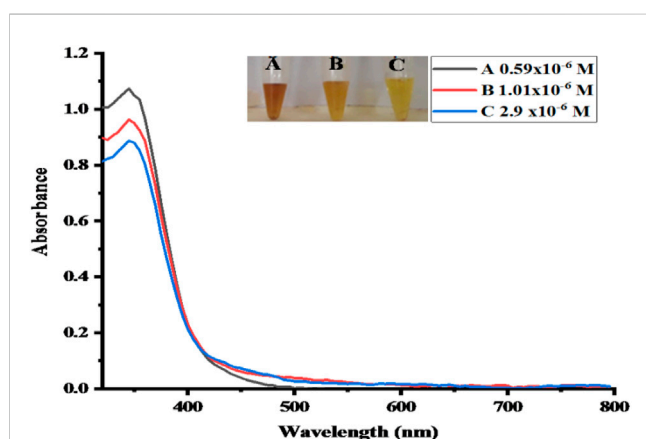

FIGURE 13
UV−Vis spectra of the real samples. Absorbance changes for **(A, B and C)** can be seen in the spectra.

in a complete color change of the mixture from brown to yellow. Therefore, pH 5 was considered optimal for the proposed sensor for further experiments. When compared to the literature, the pH value is 1.3 for the colorimetric detection of nitrite (Li et al., 2015).

3.4.3 Effect of time

The optimization of time is a key factor in biosensors. To find the optimum time for the proposed sensor, the response was examined at various time intervals ranging from 1–6 min, as shown in Figure 10. The excellent response of the proposed sensor was observed at 4 min because all the available Cuo NPs were used for the sensing of nitrite at this time. After 4 min, the color completely changed from brown to yellow. So, 4 min is the optimum time for the proposed sensor for further experiments. According to

the literature, the incubation time for the sensing of nitrite is 5 min (Daniel et al., 2009).

3.4.4 Analytical characteristics with the fabricated sensor

The analytical performance of the fabricated sensor is shown in Figure 11. The absorption peak of the proposed sensor gradually decreased with the increase in NO_2^- concentration. Under optimum conditions, with the increase in the concentration of nitrite solution, the color changes from brown to yellow, and the UV−Vis spectra are shown in Figure 11A. Using nitrite solution with a linear concentration ranging from 1×10^{-8} to 2.4×10^{-6} M at 350 nm, a drop in absorbance spectra was observed. Additionally, this probe may be utilized to accurately detect nitrate ions with a linear range of 1×10^{-8} to 2.40×10^{-6} M, with a limit of detection (LOD) of 2.69×10^{-7} M, limit of quantitation (LOQ) of 8.9×10^{-7} M, and regression coefficient (R^2) of 0.997, as shown in Figure 11B. The outcomes of the suggested assay were also evaluated using previously reported colorimetric sensors for the detection of nitrite based on various nanomaterials, as shown in Table 2. For the proposed sensor, the response time was 4 min. Furthermore, the practical performance of the proposed assay was tested on meat samples. In comparison with the previously reported sensors, the analytical results obtained from our sensor were correlated and comparable to the reported nitrite sensors (Hu et al., 2019).

3.5 Selectivity study analysis

The selectivity of the proposed biosensor was checked with other co-existing ions, such as SO_4^{2-}, CO_3^{2-}, PO_4^{3-}, Cl^-, I^-, Br^-, tar, Ca^{2+} and NO_2^-, at the same concentration of 2.40×10^{-6} M (100 μL). No colorimetric response has been observed with other ions, and only the addition of nitrite can lead to a substantial reduction in absorption at 350 nm, as shown in Figure 12. It is clearly shown that the fabricated sensor is only specific for NO_2^- determination, with an obvious color change from brown to yellow when other ions are present at an equivalent concentration, as shown in Figure 12. The sensitivity of acetic acid-coated copper oxide nanoparticles for nitrite detection is significantly higher. From the results, it is clear that the fabricated test can be used to detect nitrite specifically, both using UV−Visible spectra and the naked eye. The outcomes of the suggested assay were consistent with the published literature (Ye et al., 2015).

3.6 Real sample assay analyses

In real samples, no direct NO_2^- was detected. The proposed sensor was alternatively tested by the recovery of spiked NO_2^- solution, and standard additions, such as 0.54, 0.97, and 2.7 μM, are spiked into real samples of meat solution, as can be seen in Figure 13. It indicates that in aqueous solutions, such a method is applicable for the quantification of NO_2^-. By employing various concentrations of NO_2^- solution utilizing the optimal conditions, the actual concentration of NO_2^- in real samples is calculated using a calibrated graph that has already been produced. The obtained results with the help of percentage recovery formula are summarized in Table 3 (Nishan et al., 2021c).

Recovery % = nitrite found/nitrite added x 100 (Nishan et al., 2022).

TABLE 3 Detection of NO$_2^-$ in real samples.

Samples	Detected (µM)	Nitrite added (µM)	Nitrite found (µM)	Recovery (%)	RSD (%)
I	0.05	0.54	0.59	109.25	0.307
II	0.04	0.97	1.01	104.12	0.503
III	0.8	2.7	2.9	107.40	0.362

4 Conclusion

In the present work, a simple and inexpensive colorimetric sensor was developed for the sensing and monitoring of nitrite employing acetic acid-coated CuO nanoparticles. The fabricated sensor could selectively detect nitrite ions by a distinct color change from brown to yellow, with a limit of detection of 2.69×10^{-7} M. In the present work, no sophisticated instrumentation is required for the colorimetric response. The proposed sensor gives the best colorimetric response under optimized conditions of 100 µL of capped CuO NPs, 100 µL of nitrite solution (2.40×10^{-6} M), 4 min, and pH 5 at room temperature. We believe that the proposed sensor, under optimized conditions, will be utilized to detect and measure the nitrite and nitrate ions on the spot.

Data availability statement

The original contributions presented in the study are included in the article/Supplementary Material; further inquiries can be directed to the corresponding authors.

Author contributions

UN, SR, NM, and MA conceived the idea. MS, RU, AB, SR, JI, and NM performed the experiments. UN, HK, AM, and SA analyzed the data. UN, NM, MA, and SA wrote the manuscript. NK and IH critically evaluated the manuscript.

Conflict of interest

The authors declare that the research was conducted in the absence of any commercial or financial relationships that could be construed as a potential conflict of interest.

Publisher's note

All claims expressed in this article are solely those of the authors and do not necessarily represent those of their affiliated organizations, or those of the publisher, the editors, and the reviewers. Any product that may be evaluated in this article, or claim that may be made by its manufacturer, is not guaranteed or endorsed by the publisher.

References

Adarsh, N., Shanmugasundaram, M., and Ramaiah, D. (2013). Efficient reaction based colorimetric probe for sensitive detection, quantification, and on-site analysis of nitrite ions in natural water resources. *Anal. Chem.* 85, 10008–10012. doi:10.1021/ac4031303

Adegoke, O., Zolotovskaya, S., Abdolvand, A., and Daeid, N. N. (2021). Rapid and highly selective colorimetric detection of nitrite based on the catalytic-enhanced reaction of mimetic Au nanoparticle-CeO$_2$ nanoparticle-graphene oxide hybrid nanozyme. *Talanta* 224, 121875. doi:10.1016/j.talanta.2020.121875

Amanulla, B., Palanisamy, S., Chen, S.-M., Chiu, T.-W., Velusamy, V., Hall, J. M., et al. (2017). Selective colorimetric detection of nitrite in water using chitosan stabilized gold nanoparticles decorated reduced graphene oxide. *Sci. Rep.* 7, 14182–14189. doi:10.1038/s41598-017-14584-6

Asad, M., Muhammad, N., Khan, N., Shah, M., Khan, M., Khan, M., et al. (2022). Colorimetric acetone sensor based on ionic liquid functionalized drug-mediated silver nanostructures. *J. Pharm. Biomed. Anal.* 221, 115043. doi:10.1016/j.jpba.2022.115043

Basu, S., Ricart, K., Gladwin, M. T., Patel, R. P., and Kim-Shapiro, D. B. (2022). Tri-iodide and vanadium chloride based chemiluminescent methods for quantification of nitrogen oxides. *Nitric Oxide* 121, 11–19. doi:10.1016/j.niox.2022.01.006

Brender, J. D. (2020). "Human health effects of exposure to nitrate, nitrite, and nitrogen dioxide," in *Just enough nitrogen: Perspectives on how to get there for regions with too much and too little nitrogen*, 283–294.

Chen, J., Pang, S., He, L., and Nugen, S. R. (2016). Highly sensitive and selective detection of nitrite ions using Fe$_3$O$_4$@SiO$_2$/Au magnetic nanoparticles by surface-enhanced Raman spectroscopy. *Biosens. Bioelectron.* 85, 726–733. doi:10.1016/j.bios.2016.05.068

Cheng, Y.-H., Kung, C.-W., Chou, L.-Y., Vittal, R., and Ho, K.-C. (2014). Poly (3, 4-ethylenedioxythiophene)(PEDOT) hollow microflowers and their application for nitrite sensing. *Sens. Actuators B Chem.* 192, 762–768. doi:10.1016/j.snb.2013.10.126

Daniel, W. L., Han, M. S., Lee, J.-S., and Mirkin, C. A. (2009). Colorimetric nitrite and nitrate detection with gold nanoparticle probes and kinetic end points. *J. Am. Chem. Soc.* 131, 6362–6363. doi:10.1021/ja901609k

Deng, D., Jin, Y., Cheng, Y., Qi, T., and Xiao, F. (2013). Copper nanoparticles: Aqueous phase synthesis and conductive films fabrication at low sintering temperature. *ACS Appl. Mater. Interfaces* 5, 3839–3846. doi:10.1021/am400480k

Ethiraj, A. S., and Kang, D. J. (2012). Synthesis and characterization of CuO nanowires by a simple wet chemical method. *Nanoscale Res. Lett.* 7, 70. doi:10.1186/1556-276x-7-70

Fernández-Arias, M., Boutinguiza, M., Del Val, J., Riveiro, A., Rodríguez, D., Arias-González, F., et al. (2020). Fabrication and deposition of copper and copper oxide nanoparticles by laser ablation in open air. *Nanomaterials* 10, 300. doi:10.3390/nano10020300

Flores, M., and Toldrá, F. (2021). Chemistry, safety, and regulatory considerations in the use of nitrite and nitrate from natural origin in meat products-Invited review. *Meat Sci.* 171, 108272. doi:10.1016/j.meatsci.2020.108272

Gao, B., Zhao, X., Liang, Z., Wu, Z., Wang, W., Han, D., et al. (2020). CdS/TiO$_2$ nanocomposite-based photoelectrochemical sensor for a sensitive determination of nitrite in principle of etching reaction. *Anal. Chem.* 93, 820–827. doi:10.1021/acs.analchem.0c03315

Greer, F. R., Shannon, M., and Health, C. o. E. (2005). Infant methemoglobinemia: The role of dietary nitrate in food and water. *Pediatrics* 116, 784–786. doi:10.1542/peds.2005-1497

Hosseini-Koupaei, M., Shareghi, B., Saboury, A. A., Davar, F., Sirotkin, V. A., Hosseini-Koupaei, M. H., et al. (2019). Catalytic activity, structure and stability of proteinase K in the presence of biosynthesized CuO nanoparticles. *Int. J. Biol. Macromol.* 122, 732–744. doi:10.1016/j.ijbiomac.2018.11.001

Hosseini-Monfared, H., Parchegani, F., and Alavi, S. (2015). Carboxylic acid effects on the size and catalytic activity of magnetite nanoparticles. *J. Colloid Interface Sci.* 437, 1–9. doi:10.1016/j.jcis.2014.08.056

Hu, X., Shi, J., Shi, Y., Zou, X., Tahir, H. E., Holmes, M., et al. (2019). A dual-mode sensor for colorimetric and fluorescent detection of nitrite in hams based on carbon dots-neutral red system. *Meat Sci.* 147, 127–134. doi:10.1016/j.meatsci.2018.09.006

Jaiswal, N., Tiwari, I., Foster, C. W., and Banks, C. E. (2017). Highly sensitive amperometric sensing of nitrite utilizing bulk-modified MnO$_2$ decorated Graphene oxide nanocomposite screen-printed electrodes. *Electrochim. Acta* 227, 255–266. doi:10.1016/j.electacta.2017.01.007

Karrat, A., Digua, K., and Amine, A. (2022). Development of a simplified spectrophotometric method for nitrite determination in water samples. *Spectrochim. Acta Part A Mol. Biomol. Spectrosc.* 267, 120574. doi:10.1016/j.saa.2021.120574

Kumar, V. V., and Anthony, S. P. (2014). Highly selective silver nanoparticles based label free colorimetric sensor for nitrite anions. *Anal. Chim. Acta* 842, 57–62. doi:10.1016/j.aca.2014.06.028

Lanje, A. S., Sharma, S. J., Pode, R. B., and Ningthoujam, R. S. (2010). Synthesis and optical characterization of copper oxide nanoparticles. *Adv. Appl. Sci. Res.* 1, 36–40.

Li, T., Li, Y., Zhang, Y., Dong, C., Shen, Z., and Wu, A. (2015). A colorimetric nitrite detection system with excellent selectivity and high sensitivity based on Ag@Au nanoparticles. *Analyst* 140, 1076–1081. doi:10.1039/c4an01583e

Lim, H. S., Lee, S. J., Choi, E., Lee, S. B., Nam, H. S., and Lee, J. K. (2022). Development and validation of an ionic chromatography method for nitrite determination in processed foods and estimation of daily nitrite intake in Korea. *Food Chem.* 382, 132280. doi:10.1016/j.foodchem.2022.132280

Lin, A.-J., Wen, Y., Zhang, L.-J., Lu, B., Li, Y., Jiao, Y.-Z., et al. (2011). Layer-by-layer construction of multi-walled carbon nanotubes, zinc oxide, and gold nanoparticles integrated composite electrode for nitrite detection. *Electrochim. acta* 56, 1030–1036. doi:10.1016/j.electacta.2010.10.058

Loganathan, S., Valapa, R. B., Mishra, R. K., Pugazhenthi, G., and Thomas, S. (2017). "Thermogravimetric analysis for characterization of nanomaterials," in *Thermal and rheological measurement techniques for nanomaterials characterization* (Elsevier), 67–108.

Majou, D., and Christieans, S. (2018). Mechanisms of the bactericidal effects of nitrate and nitrite in cured meats. *Meat Sci.* 145, 273–284. doi:10.1016/j.meatsci.2018.06.013

Nam, Y.-S., Noh, K.-C., Kim, N.-K., Lee, Y., Park, H.-K., and Lee, K.-B. (2014). Sensitive and selective determination of NO$_2^-$ ion in aqueous samples using modified gold nanoparticle as a colorimetric probe. *Talanta* 125, 153–158. doi:10.1016/j.talanta.2014.02.030

Nam, J., Jung, I.-B., Kim, B., Lee, S.-M., Kim, S.-E., Lee, K.-N., et al. (2018). A colorimetric hydrogel biosensor for rapid detection of nitrite ions. *Sens. Actuators B Chem.* 270, 112–118. doi:10.1016/j.snb.2018.04.171

Nishan, U., Gul, R., Muhammad, N., Asad, M., Rahim, A., Shah, M., et al. (2020). Colorimetric based sensing of dopamine using ionic liquid functionalized drug mediated silver nanostructures. *Microchem. J.* 159, 105382. doi:10.1016/j.microc.2020.105382

Nishan, U., Sabba, U., Rahim, A., Asad, M., Shah, M., Iqbal, A., et al. (2021a). Ionic liquid tuned titanium dioxide nanostructures as an efficient colorimetric sensing platform for dopamine detection. *Mater. Chem. Phys.* 262, 124289. doi:10.1016/j.matchemphys.2021.124289

Nishan, U., Haq, S. U., Rahim, A., Asad, M., Badshah, A., Ali Shah, A.-u.-H., et al. (2021b). Ionic-Liquid-Stabilized TiO2 nanostructures: A platform for detection of hydrogen peroxide. *ACS Omega* 6, 32754–32762. doi:10.1021/acsomega.1c04548

Nishan, U., Niaz, A., Muhammad, N., Asad, M., Khan, N., Khan, M., et al. (2021c). Non-enzymatic colorimetric biosensor for hydrogen peroxide using lignin-based silver nanoparticles tuned with ionic liquid as a peroxidase mimic. *Arabian J. Chem.* 14, 103164. doi:10.1016/j.arabjc.2021.103164

Nishan, U., Khan, H. U., Rahim, A., Asad, M., Qayum, M., Khan, N., et al. (2022). Non-enzymatic colorimetric sensing of nitrite in fortified meat using functionalized drug mediated manganese dioxide. *Mater. Chem. Phys.* 278, 125729. doi:10.1016/j.matchemphys.2022.125729

Odedairo, T., Chen, J., and Zhu, Z. (2013). Metal–support interface of a novel Ni–CeO$_2$ catalyst for dry reforming of methane. *Catal. Commun.* 31, 25–31. doi:10.1016/j.catcom.2012.11.008

Ozdestan, O., and Uren, A. (2010). Development of a cost-effective method for nitrate and nitrite determination in leafy plants and nitrate and nitrite contents of some green leafy vegetables grown in the Aegean region of Turkey. *J. Agric. food Chem.* 58, 5235–5240. doi:10.1021/jf904558c

Pourreza, N., and Abdollahzadeh, R. (2019). Colorimetric determination of hydrazine and nitrite using catalytic effect of palladium nanoparticles on the reduction reaction of methylene blue. *Microchem. J.* 150, 104067. doi:10.1016/j.microc.2019.104067

Qu, J., Dong, Y., Wang, Y., and Xing, H. (2015). A novel sensor based on Fe3O4 nanoparticles–multiwalled carbon nanotubes composite film for determination of nitrite. *Sens. Bio-Sens. Res.* 3, 74–78. doi:10.1016/j.sbsr.2014.10.009

Rajaji, U., Manavalan, S., Chen, S.-M., Chinnapaiyan, S., Chen, T.-W., and Ramalingam, R. J. (2019). Facile synthesis and characterization of erbium oxide (Er$_2$O$_3$) nanospheres embellished on reduced graphene oxide nanomatrix for trace-level detection of a hazardous pollutant causing Methemoglobinaemia. *Ultrason. Sonochem.* 56, 422–429. doi:10.1016/j.ultsonch.2019.02.023

Sáenz-Galindo, A., López-López, L. I., Fabiola, N., Castañeda-Facio, A. O., Rámirez-Mendoza, L. A., Córdova-Cisneros, K. C., et al. (2018). "Applications of carboxylic acids in organic synthesis, nanotechnology and polymers," in *Carboxylic acid: Key role in life sciences*, 35.

Sarkar, A., Kapoor, S., and Mukherjee, T. (2005). Synthesis of silver nanoprisms in formamide. *J. colloid interface Sci.* 287, 496–500. doi:10.1016/j.jcis.2005.02.017

Shi, W.-Z., Liang, Y.-S., Lu, B., Chen, M., Li, Y., and Yang, Z. (2019). Cuprous oxide nanoparticles: Preparation and evaluation of antifouling activity. *Quím. Nova* 42, 638–641. doi:10.21577/0100-4042.20170374

Singh, P., Singh, M. K., Beg, Y. R., and Nishad, G. R. (2019). A review on spectroscopic methods for determination of nitrite and nitrate in environmental samples. *Talanta* 191, 364–381. doi:10.1016/j.talanta.2018.08.028

Sun, X., and Luo, Y. (2005). Preparation and size control of silver nanoparticles by a thermal method. *Mater. Lett.* 59, 3847–3850. doi:10.1016/j.matlet.2005.07.021

Teles, A. R. R., Capela, E. V., Carmo, R. S., Coutinho, J. A., Silvestre, A. J., and Freire, M. G. (2017). Solvatochromic parameters of deep eutectic solvents formed by ammonium-based salts and carboxylic acids. *Fluid Phase Equilib.* 448, 15–21. doi:10.1016/j.fluid.2017.04.020

Wang, J., Zhao, D., Zhang, Y., Li, J., and Xu, C. (2014). A highly sensitive sensor for the detection of nitrite based on a nanoporous Fe$_2$O$_3$–CoO composite. *Anal. Methods* 6, 3147–3151. doi:10.1039/c4ay00171k

Wang, X., Hu, Y., and Wei, H. (2016). Nanozymes in bionanotechnology: From sensing to therapeutics and beyond. *Inorg. Chem. Front.* 3, 41–60. doi:10.1039/c5qi00240k

Xiong, Y., Li, M., Liu, H., Xuan, Z., Yang, J., and Liu, D. (2017). Janus PEGylated gold nanoparticles: A robust colorimetric probe for sensing nitrite ions in complex samples. *Nanoscale* 9, 1811–1815. doi:10.1039/c6nr07879f

Ye, Y., Guo, Y., Yue, Y., and Zhang, Y. (2015). Facile colorimetric detection of nitrite based on anti-aggregation of gold nanoparticles. *Anal. Methods* 7, 4090–4096. doi:10.1039/c5ay00386e

Zhang, J., Yang, C., Wang, X., and Yang, X. (2012). Colorimetric recognition and sensing of nitrite with unmodified gold nanoparticles based on a specific diazo reaction with phenylenediamine. *Analyst* 137, 3286–3292. doi:10.1039/c2an35204d

Zhang, K., Hu, Y., and Li, G. (2013). Diazotization-coupling reaction-based selective determination of nitrite in complex samples using shell-isolated nanoparticle-enhanced Raman spectroscopy. *Talanta* 116, 712–718. doi:10.1016/j.talanta.2013.07.019